HHS Public Access

Author manuscript

Liver Transpl. Author manuscript; available in PMC 2018 May 17.

Published in final edited form as:

Liver Transpl. 2015 April ; 21(4): 442–453. doi:10.1002/lt.24057.

Noninvasive 3D imaging of liver regeneration in a mouse model of hereditary tyrosinemia type 1 using the sodium iodide symporter gene

Raymond D. Hickey[1,2,*], **Shennen A. Mao**[2], **Bruce Amiot**[2], **Lukkana Suksanpaisan**[3], **Amber Miller**[1], **Rebecca Nace**[1], **Jaime Glorioso**[2], **Kah Whye Peng**[1], **Yasuhiro Ikeda**[1], **Stephen J. Russell**[1,#], and **Scott L. Nyberg**[2,#]

[1]Department of Molecular Medicine, Mayo Clinic, Rochester, MN, USA

[2]Department of Surgery, Mayo Clinic, Rochester, MN, USA

[3]Imanis Life Sciences, Rochester, MN, USA

Abstract

Cell transplantation is a potential treatment for the many liver disorders that are currently only curable by organ transplantation. However, until now there has been no report of a clinically-relevant method to image transplanted hepatocytes both noninvasively and longitudinally after transplantation. We hypothesized that the thyroidal sodium iodide symporter (NIS) gene could be used to visualize transplanted hepatocytes in a rodent model of inherited liver disease, hereditary tyrosinemia type 1. Wildtype C57Bl/6J mouse hepatocytes were transduced ex vivo using a lentiviral vector containing the mouse *Slc5a5* (NIS) gene under the control of the thyroxine-binding globulin promoter. NIS-labeled cells could robustly concentrate radiolabeled iodine in vitro, with lentiviral transduction efficiencies greater than 80% achieved in the presence of dexamethasone. Next, NIS-labeled hepatocytes were transplanted into congenic fumarylacetoacetate hydrolase knockout ($Fah^{-/-}$) mice, resulting in prevention of liver failure. NIS-labeled hepatocytes were readily imaged in vivo by single-photon emission computed tomography, demonstrating for the first time noninvasive 3D imaging of regenerating tissue in individual animals over time using clinically relevant methodology. We also tested the efficacy of primary hepatocyte spheroids to engraft in the liver. Using the NIS-reporter, robust spheroid engraftment and survival could be detected longitudinally after direct parenchymal injection, thereby demonstrating a novel strategy for hepatocyte transplantation.

Conclusion—This work is the first to demonstrate the efficacy of NIS-imaging in the field of liver regeneration. We anticipate that NIS-labeling will allow non-invasive identification of hepatocytes and stem cells in both preclinical models of liver disease and clinical cell transplantation studies.

Keywords

hepatocyte transplantation; cell therapy; fumarylacetoacetate hydrolase; imaging; NIS

[*]To whom correspondence should be addressed, **Contact Information** Raymond Hickey, Ph.D., Mayo Clinic, 200 First Street SW, Rochester, MN 55905, Tel 507.283.0878, Fax 507.284.8388, hickey.raymond@mayo.edu.

[#]Joint senior authors.

INTRODUCTORY STATEMENT

An alternative strategy to orthotopic liver transplantation is cell transplantation. A number of small animal models of metabolic liver diseases have been treated by hepatocyte transplantation. The first published partial correction of a metabolic disorder in humans was performed by Fox and colleagues in a patient with Crigler–Najjar syndrome type 1.(1) Since then a number of patients with metabolic disorders have undergone hepatocyte transfusions with encouraging, albeit modest, success (reviewed in (2)). More recently, a number of alternative cell therapy strategies for liver disease have been attempted, including transplantation of pluripotent stem cells, liver stem cells, directly differentiated hepatocyte-like cells, and mesenchymal stem cells (reviewed in (3, 4)). One major limitation of current transplantation procedures is an inability to monitor cells noninvasively and longitudinally after infusion.(5) This current limitation is all the more important based on recent studies demonstrating extended periods of time, often up to six months, for complete differentiation of stem cells to occur *in vivo*.(6, 7) Additionally, the ability of hepatocytes to engraft and expand outside of the liver (8) requires that an appropriate method to accurately identify the location of transplanted cells. Noninvasive, longitudinal molecular imaging, therefore, will play an essential part in not only identifying transplanted cells, but also helping to decipher the fate and differentiation of transplanted stem cells.

The thyroidal sodium iodide symporter (NIS) reporter gene (*Slc5a5*) is a promising candidate for this purpose, not only in preclinical animal model studies, but also in clinical hepatocyte transplantations as this reporter has already been tested in other clinical human studies (reviewed in (9)). NIS is an intrinsic plasma membrane glycoprotein that co-transports two sodium ions down the electrochemical gradient and one iodide ion up the electrochemical gradient from the plasma into the cell. NIS is normally expressed in thyroid follicular cells, stomach surface epithelium and salivary gland ductal cells with minimal expression in the liver. Upon addition of radiolabelled iodine (e.g. I^{125}) or technetium pertechnetate (an iodide analog) *in vitro* or *in vivo*, NIS-expressing cells can uptake the radiolabel, allowing both qualitative and quantitative analysis of NIS-expressing cells by single-photon emission computed tomography (SPECT) or positron emission tomography (PET).(10) A key advantage to NIS imaging is that it is noninvasive, and can be performed longitudinally to track hepatocyte engraftment, survival and expansion.

In humans, hereditary tyrosinemia type 1 (HT1) is a severe, autosomal recessive inborn error of metabolism caused by deficiency of fumarylacetoacetate hydrolase (FAH), a metabolic enzyme that catalyzes the last step of tyrosine metabolism.(11) *Fah*-knockout ($Fah^{-/-}$) mice have been used as a small animal model for hepatocyte transplantation.(12, 13) In this model, engrafted FAH-positive cells have a selective growth advantage and can repopulate the $Fah^{-/-}$ liver in the absence of NTBC. However, to date there has been no demonstration of a clinically-relevant imaging modality to monitor the fate of transplanted hepatocytes longitudinally in individual animals. In the present study, we used $Fah^{-/-}$ mice to test the hypothesis that NIS-labeled hepatocytes can be monitored noninvasively after transplantation using SPECT to assess their repopulation in individual mice over time.

EXPERIMENTAL PROCEDURES

Plasmid construction

pSIN-CSGWdlNotl-based lentiviral vectors were produced from the parent vector pSIN-CSGWdlNotl-SFFV-EGFP that contained the EGFP transgene under the control of the spleen focus forming virus (SFFV) promoter.(14) Initially, the SFFV promoter was replaced with a construct that contained two copies of a human α1-microglobulin/bikunin enhancer and the promoter from the human thyroid hormone-binding globulin (TGB) gene.(15, 16) Subsequently, the mouse *Slc5a5* cDNA(17) was cloned into the TBG vector in place of EGFP to produce the LV-TBG-NIS expression construct. In order to generate viral vectors, the LV-TBG-NIS expression construct, along with the packaging plasmid pCMVR8.91(18) and the vesicular stomatitis virus glycoprotein G (VSV-G)-expressing plasmid, pMD.G,(18) were transiently transfected into 293 cells using Fugene6 (Roche, Indianapolis, IN). Transfected cells were washed after 16 hours, and grown for another 48 hours, after which supernatants were harvested and passed through a 0.45-μm filter. Vector supernatants were concentrated by ultracentrifugation (25,000RPM, 1.5 hours at 4°C), and resuspended in serum-free media (OptiMEM, Life Technologies, Grand Island, CA), aliquoted, and stored at −80°C.

Animals and animal care

All animals received humane care in compliance with the regulations of the Institutional Animal Care and Use Committee at Mayo Clinic. Donor C57Bl/6J mice (Stock # 000664) were purchased from the Jackson Laboratories. Recipient $Fah^{-/-}$ mice(13) on the C57Bl/6J background were administered NTBC (Yecuris, Portland, OR) in the drinking water at 8 mg/L to prevents acute liver injury prior to transplantation.

Lentiviral transduction optimization

The lentiviral vector LV-SFFV-EGFP was transduced into primary mouse hepatocytes at a MOI of 10. Media was changed every two days, and cells were analyzed for GFP expression by flow cytometry after five days. To dissociate cells into a single cell suspension, 0.05% Tryspin/EDTA was used. Cells were washed and fixed in 1% paraformaldehyde for 15 min prior to analysis on a FACSCalibur (BD Biosciences, San Jose, CA). Data were analyzed using FlowJo (Treestar, Ashland, OR).

In vitro iodine uptake assay

The lentiviral vector LV-TBG-NIS was transduced into primary mouse hepatocytes in a 12-well tissue culture plate at a MOI of 10. Media was changed every two days, and cells were assayed for the ability to uptake radiolabeled iodine after five days, as previously described.(19) Briefly, cells were washed with Hanks' Balanced Salt solution (HBSS; Sigma-Aldrich, St. Louis, MI) containing 10mM HEPES and incubated with an activity of 1×10^5 cpm NaI(^{125}I)/0.1 mL in 1 mL HBSS containing HEPES. 100μM KClO4 was added to inhibit NIS-mediated iodide influx in control wells. Plates were incubated at 37°C for 45 minutes. Cells were washed twice with ice-cold HBSS containing HEPES buffer. Cells were lysed

with 1M NaOH and the activity was determined by γ-counting. All data points were measured in triplicate and displayed as means ± SEM.

SPECT/CT imaging system

Imaging was performed in the Mayo Clinic Small Animal Imaging Core using a U-SPECT-II/CT scanner (MILabs, Utrecht, The Netherlands)(20). Scan-volumes for both the SPECT and CT were selected based on orthogonal optical images provided by integrated webcams. Micro-CT image acquisition was performed in 4 min for normal resolution (169-μm square voxels, 640 slices) at 0.5 mA and 60 kV. Image acquisition time was approximately 20 minutes for SPECT (24 projections at 50 seconds per bed position). All pinholes focus on a single volume in the center of the tube and by using an XYZ stage large volumes up to the entire animal can be scanned at uniform resolution.(21) Coregistration of the SPECT and CT images was performed by applying pre-calibrated spatial transformation to the SPECT images to match with the CT images. In order to mask background signal from the stomach, animals were administered 350 μl undiluted barium sulfate (40% w/v, Tagitol V, E-Z-EM, Lake Success, NY, USA) by oral gavage using a 22-gauge plastic feeding tube (Instech Laboratories, Plymouth, PA, USA), as previously described.(22)

Image reconstruction and data processing

SPECT reconstruction was performed using a POSEM (pixel-based ordered subset expectation maximization) algorithm(23) with 6 iterations and 16 subsets. CT data were reconstructed using a Feldkamp cone beam algorithm (NRecon v1.6.3, Skyscan). After reconstruction, SPECT images were automatically registered to the CT images according to the pre-calibrated transformation, and resampled to the CT voxel size. Co-registered images were further rendered and visualized using the PMOD software (PMOD Technologies, Zurich, Switzerland). A 3D-Guassian filter (0.8 mm FWHM) was applied to suppress noise, and LUTs were adjusted for good visual contrast. Reconstructed images were visualized as both orthogonal slices and maximum intensity projections. Maximal intensity projection videos and three-dimensional rendering of regions of interests were performed on the PMOD software.

Histology and biochemical analysis

For histology analysis, tissue samples were fixed in 10% neutral buffered formalin (Protocol, Fisher-Scientific, Pittsburgh, PA) and processed for paraffin embedding and sectioning. For hematoxylin and eosin staining, slides were prepared using standard protocols. FAH immunohistochemistry using a polyclonal rabbit anti-FAH primary antibody(24) was performed with a Bond III automatic stainer (Leica, Buffalo Grove, IL) with a 20 min antigen retrieval step using Bond Epitope Retrieval Solution 2 (Leica, Buffalo Grove, IL) and stained with diaminobenzidine (Leica, Buffalo Grove, IL)For biochemical analysis of alkaline phosphatase, alanine aminotransferase and total bilirubin, plasma was analyzed using the VetScan VS2 benchtop analyzer (Mammalian Liver Profile; Abaxis, Union City, CA) according to the manufacturer’s instructions.

Hepatocyte transplantation

Hepatocytes were harvested using a typical two-step collagenase perfusion technique, as previously described.(25) The number and viability of cells were determined by trypan blue exclusion. 0.5×10^6 cells were plated into six-well Primaria culture plates (BD Biosciences, San Jose, CA) containing the following media: DMEM (Thermo Fisher Scientific, Waltham, MA); 10% heat-inactivated FBS (Corning, Herndon, VA); 10mM HEPES (Corning, Herndon, VA); Penicillin/Streptomycin (Corning, Herndon, VA). Fresh media was replaced two hours later that contained 10uM dexamethasone (Sigma-Aldrich, St. Louis, MI) and 10ng/ml EGF (Sigma-Aldrich, St. Louis, MI). Lentiviral vectors were added to the media at a multiplicity of infection that was determined by p24 ELISA (Clontech, Mountain View, CA). Hepatocytes were harvested the following day using 0.05% Tryspin/EDTA (Corning, Herndon, VA). The number and viability of cells were determined by trypan blue exclusion. Hepatocytes were resuspended in a volume of 100µl growth media containing 2µg/ml of DNaseI (Sigma-Aldrich, St. Louis, MI) to minimize clumping of cells. Cells were injected via the spleen using standard intrasplenic injection protocols. (26)

Primary hepatocyte spheroids

Freshly isolated hepatocytes were suspended in Williams-E medium supplemented with 10% FBS, 10 U/mL penicillin G, 100 µg/mL streptomycin, 10 µg/mL insulin, 5.5 µg/mL transferrin, 5 ng/mL sodium selenite at a concentration 1×10^6 viable cells/mL. Hepatocyte suspensions of 20mL were inoculated into spheroid dishes (10 × 8 × 2 cm) custom-made with glass and siliconized with Sigmacote. Spheroid dishes were placed in the 37°C incubator with 5% CO2 and rocked continuously at 10 cycles per minute for 48 hours to induce spheroid formation.

RESULTS

Lentiviral-mediated transgene expression is increased in the presence of dexamethasone

In future clinical studies, efficient ex vivo hepatocyte transduction protocols will be required in order for ex vivo hepatocyte gene therapy to be successful. Rodent hepatocytes, in particular, are resistant to lentiviral transduction with transduction efficiencies of <50% commonly reported. However, recent progress has been made by including growth factors such as epidermal growth factor (EGF) in transduction media that have allowed higher transduction efficiencies to be achieved.(27) We initially tested the effect of EGF on lentiviral transduction using a lentiviral vector expressing EGFP under the control of the ubiquitous spleen focus forming virus (SFFV) promoter but we did not detect a significant difference in EGFP+ cells that contained EGF in the transduction media (Figure 1A and S1). Next, we added dexamethasone to the media and noticed a significant increase in EGFP+ cells, which was independent of EGF. Based on these results, lentiviral transduction of primary hepatocytes was performed in the presence of dexamethasone and EGF for the remaining experiments.

NIS-labeled mouse hepatocytes can concentrate radiolabeled iodine in vitro

It is unknown whether hepatocytes have the ability to concentrate iodine if NIS is exogenously expressed. Using our optimized transduction protocol, primary hepatocytes were transduced with a lentiviral vector expressing NIS under the control of a liver specific promoter (LV-TBG-NIS; see Experimental Procedures for details). Hepatocytes were cultured for five days, after which the ability of these cells to take up iodine intracellularly was assessed using I-125 (Figure 1B). NIS-labeled hepatocytes had significantly increased uptake of radioisotope compared to non-transduced hepatocytes when I-125 was added to the media for 45 minutes. Importantly, the ability of NIS-labeled hepatocytes to concentrate radioisotope was significantly abrogated by the addition of the NIS competitive inhibitor potassium perchlorate in the media, indicating expression of NIS was responsible for increased radioisotope uptake in transduced hepatocytes.

NIS-labeled mouse hepatocytes can concentrate radiolabeled iodine in vivo

Transplanted FAH+ hepatocytes have a selective growth advantage over resident *Fah*$^{-/-}$ hepatocytes when mice are taken off the protective drug NTBC.(28) As a pilot experiment, primary hepatocytes from FAH+ wildtype mice were isolated and labeled with LV-TBG-NIS prior to transplantation into *Fah*$^{-/-}$ mice (Fig. 2). As a control, non-NIS labeled hepatocytes were also transplanted into *Fah*$^{-/-}$ mice. Mice underwent NTBC withdrawal and selection and SPECT/CT imaging using technetium-99m-pertechnetate was performed after twelve weeks. In a control animal transplanted with hepatocytes not labeled with NIS, isotope uptake was not detected in the liver (Figure 3A & Supplementary Video 1). In contrast, in a mouse transplanted with NIS-labeled hepatocytes, robust uptake of isotope was visible in the liver of these animals, confirming repopulation of the host liver with NIS-labeled cells (Figure 3A, B & Supplementary Video 2). Finally, SPECT imaging indicated that repopulation of the liver by donor hepatocytes was not uniform (Figure 3B). In order to confirm this histologically, FAH-immunohistochemistry was performed. Consistent with the imaging data, FAH+ cells were detected non-uniformly throughout the liver (Figure 3C).

NIS-imaging permits longitudinal 3D imaging of repopulating hepatocytes in Fah$^{-/-}$ livers

We next set out to determine if SPECT/CT imaging could be used to quantitatively monitor repopulation kinetics longitudinally in individual mice. Mice were transplanted intrasplenically with 5×10^4 hepatocytes labeled with LV-TBG-NIS. Animals underwent NTBC selection and SPECT/CT imaging using technetium-99m-pertechnetate was performed at two different time points: after 41 and 85 days of NTBC selection. In this group of four mice (numbered 160.01, 160.10, 160.20 and 160.30), there was a statistically significant increase in radiolabel uptake over the two time points (Figure 4A), consistent with previous data that FAH+ cells can expand in the *Fah*$^{-/-}$ liver. Additionally, this increase in liver uptake could be directly visualized at the two time points, revealing expansion of individual cell clusters over time throughout the livers of single animals (Figure 4B). The general shape and location of nodules was consistent overtime, but size and uptake intensity increased, indicating expansion of cells. Furthermore SPECT/CT imaging was able to resolve individual nodules of transplanted cells. Analysis of serial SPECT/CT sections demonstrated distinct nodules increasing and then decreasing in nodule diameter and uptake

intensity, revealing that individual nodule geometry is most similar to spherical geometry (Figure 5).

NIS-labeling of hepatocytes does not impact hepatocyte function in vivo

As NIS is not normally expressed in the liver, we asked the question as to whether forced expression of NIS in hepatocytes would impact negatively liver function in transplanted mice. In the absence of transplanted hepatocytes, *Fah*$^{-/-}$ mice die of acute liver failure when the protective drug NTBC is removed from their drinking water.(13, 29) Transplantation and expansion of NIS-labeled hepatocytes (Figure 4) did not impact negatively the rescue of liver failure in *Fah*$^{-/-}$ mice. After NTBC withdrawal, mice survived long term and continued to gain weight over time compared to non-transplanted controls (data not shown). Histologically, the livers of transplanted mice appeared normal, and in contrast to *Fah*$^{-/-}$ mice off NTBC, there was no evidence of profound hepatocyte damage typically seen in *Fah*$^{-/-}$ mice off NTBC (Figure 6A–C). Consistent with the histological data, biochemical analysis of plasma indicated no significant liver damage in NIS-labeled hepatocyte transplanted mice (Figure 6D–F). Similar to *Fah*$^{-/-}$ mice on NTBC, transplanted mice has significantly reduced levels of alkaline phosphatase, alanine aminotransferase, and total bilirubin compared to *Fah*$^{-/-}$ mice off NTBC.

NIS-labeling enables noninvasive imaging of hepatocyte spheroid engraftment in vivo

It has been previously demonstrated that primary hepatocyte spheroids can be formed using a rocking suspension technique.(30, 31) While culture of hepatocytes as spheroids has been shown to maintain cellular function better than other in vitro culture methods,(32) engraftment has not been demonstrated in a mouse model of metabolic disease. We initially tested whether pig hepatocytes could be transduced by lentiviral vectors during spheroid formation using vectors expressing either GFP (LV-TBG-GFP) or NIS (LV-TBG-NIS) under control of the TBG promoter. Robust GFP+ expression could be detected in LV-TBG-GFP transduced cells after formed spheroids were plated as a monolayer (Figure 7A). Additionally, LV-TBG-NIS-transduced cells were able to uptake radiolabelled iodine in vitro (Figure 7B). Next, wild-type mouse hepatocytes from a C57Bl6/6J donor were rocked in vitro for 48 hours in the presence of LV-TBG-NIS. Hepatocyte spheroids were formed that had an average diameter of 60um. These spheroids were injected directly into the liver parenchyma of recipient *Fah*$^{-/-}$ mice and SPECT/CT imaging used to identify and monitor cells longitudinally. Mice were imaged 13 days and 28 days after transplantation, revealing a consistent and specific focus of radiolabel uptake at the site of injection (Figure 7C & S2A). Subsequently, FAH-immunohistochemistry was performed to confirm detection of donor cells, revealing FAH+ transplanted spheroids had integrated normally into the parenchyma of the *Fah*$^{-/-}$ liver (Figure 7D & S2B).

DISCUSSION

In the current study, we tested the ability of the NIS reporter gene to be used to monitor hepatocyte repopulation in a mouse model of HT1 using SPECT/CT imaging. While it has been previously demonstrated that donor FAH+ hepatocytes that engraft have a proliferative advantage over host FAH-hepatocytes,(12) to date there has been no demonstration of a

clinically-relevant imaging modality to monitor the fate of transplanted hepatocytes longitudinally. In order to label hepatocytes with the reporter gene, we used a lentiviral vector expressing NIS under the control of a liver specific promoter to permanently label the cells through lentiviral-mediated integration of the transgene. Labeled hepatocytes were transplanted by intrasplenic injection and SPECT/CT imaging was performed longitudinally to quantitatively and qualitatively assess hepatocyte repopulation. Repopulation kinetics were similar to those previously published,(24) and NIS labeling did not have any negative effect on hepatocyte biology, and repopulated mice were rescued from acute liver failure caused by FAH deficiency.(29)

A number of imaging modalities have been used to visualize cells in vivo, including fluorescence imaging, bioluminescence imaging, SPECT, PET, and magnetic resonance imaging (reviewed in (33)). The most common method to image cells in a small animal is the use of the luciferase reporter gene for bioluminescence imaging.(34) While this method has been shown to label various cell types in vivo, including hepatocytes,(35, 36) its more widespread use is limited by a number of critical factors, including limited resolution, elicitation of an immune response against the foreign transgene, and an inability to image fluorescence in deep tissue (>2cm), particularly relevant to the liver.(37, 38) As better preclinical large animal models become available,(39–41) the ability to perform noninvasive in vivo imaging will be critical for several aspects of regenerative medicine, including gene therapy and cell therapy. Therefore, while luciferase imaging will continue to be an acceptable modality for in vivo imaging in small animals, alternative in vivo imaging protocols will be required for preclinical studies in larger animals. An alternative strategy is to label hepatocytes prior to transplantation with a radionuclide, such as the inert metal indium-111 (^{111}In)-oxine. Using this method, it has been demonstrated that hepatocytes can incorporate ^{111}In, allowing in vivo SPECT imaging to identify the biodistribution of transplanted cells.(42, 43) Initial studies in mice and rats have now been replicated in human studies.(44, 45) However, while this method clearly demonstrates efficacy and safety of SPECT imaging using a radionuclide, it is limited by three key factors: only short term imaging is possible as the radiolabel is lost within days, hepatocyte labeling efficiencies are low, and detection of ^{111}In is independent of cell viability.

NIS imaging has a number of advantages for noninvasive imaging for future preclinical and clinical studies for cell therapy for metabolic liver disease. First, no immune response was apparent in these studies based on long term detection of NIS-positive cells, confirming previous reports of non-immunogenicity with this reporter gene and consistent with the fact that NIS is normally expressed in several cell types in the body, including the thyroid and stomach.(9) Second, the NIS cDNA is small enough (<3kb mRNA) that in addition to use in lentiviral vectors, NIS has the ability to be cloned into various vectors, including those with small packaging capacities such as adeno-associated virus. Third, SPECT and PET imaging will be necessary for deep tissue penetration to detect transplanted cells in preclinical models, such as pig,(46) as well as human clinical trials.(47) This is a critical disadvantage of luciferase reporter imaging that is unlikely to be overcome. Fourth, SPECT imaging can be performed longitudinally for months, and potentially years, when cells are labeled with an integrated gene like NIS. This is in contrast to ^{111}In labeling, which is a useful parameter to monitor short term biodistribution of cells, but cannot be used for long term studies.(45)

Fifth, while it was not possible to directly compare luciferase and SPECT imaging directly in these experiments, the resolution at which SPECT/CT could identify individual nodules of FAH+ cells was superior to any previously published data that used luciferase for hepatocyte imaging.(48, 49) Finally, NIS could be used as a suicide gene to provide an additional safety mechanism for clinical cell therapies. To date, genes such as herpesvirus thymidine kinase(50) and iCasp9(51) has been used; however, those genes can be immunogenic and can induce undesired immune responses upon cell transplantation. In contrast, NIS gene facilitates arming with a non-immunogenic suicide mechanism upon treatment with I^{131}.

Using NIS as a reporter, we were able to demonstrate for the first time engraftment and survival of primary hepatocyte spheroids after direct injection into the parenchyma. Since initial preclinical experiments in a rodent model for Crigler-Najjar syndrome type 1, a number of small animal models of metabolic liver diseases have been treated by hepatocyte transplantation.(28, 52, 53). These animal experiments have paved the way for a number of human hepatocyte transplantations to occur, including the first published partial correction in a patient with metabolic liver disease in 1998 (1, 5). However, one of the primary limitations of hepatocyte transplantation is the low efficiency of cell engraftment. Different strategies have been proposed to improve engraftment, including conditioning of the donor liver,(54) and grafting of cells embedded in biomaterials.(35) It has been previously demonstrated that rat hepatocyte spheroids formed by rocked technique maintain differentiated hepatocyte gene expression and function.(32) The data presented here builds upon those studies by demonstrating a potential new strategy for hepatocyte transplantation. Additionally, maintenance of hepatocyte function in vitro will be a critical component for ongoing ex vivo gene correction strategies. Therefore, culture of hepatocytes as spheroids may provide a novel resource for future gene therapy protocols.

In conclusion, using a clinically relevant imaging modality, we were able to monitor for the first time the fate of transplanted hepatocytes in a small animal model of metabolic disease. NIS-labeled hepatocytes allowed high-resolution imaging of individual clusters of cells, and these cells could be longitudinally monitored in individual animals using the simple and safe imaging modality SPECT. Importantly, NIS-imaging had no impact on hepatocyte function or replication capacity, thereby implying it will be an ideal candidate for future clinical hepatocyte transplantations. To this point, nuclear imaging using SPECT or PET has already taken place safely and efficaciously in a number of clinical trials for cancer studies.(47) Based on these findings, the use of NIS labelling for nuclear imaging of cell transplantation therapies is warranted.

Supplementary Material

Refer to Web version on PubMed Central for supplementary material.

Acknowledgments

We wish to thank Markus Grompe (Oregon Health & Science University, Portland, OR) for generously providing *Fah*$^{-/-}$ mice for use in this study. Funding for importing mice was provided by the Center for Cell Signaling in Gastroenterology at Mayo Clinic. We thank LouAnn Gross (Mayo Clinic, Rochester) and Jenny Pattengill (Mayo

Clinic, Scottsdale, AZ) for histology support and Tracy Decklever and Dianna Glynn (Mayo Clinic, Rochester) for SPECT/CT imaging.

Financial Support

RDH was funded by the Center for Regenerative Medicine at Mayo Clinic, a NIH T32 training grant (DK007198), an American Liver Foundation Postdoctoral Fellowship Award. SLN was funded by the Wallace H. Coulter Foundation, and the American Society of Transplant Surgeons/Pfizer Collaborative Scientist Grant. AM was supported by the Mayo Clinic Gary and Anita Klesch Predoctoral Fellowship and the Mayo CCaTS from the National Center for Advancing Translational Sciences (UL1TR000135).

List of Abbreviations

CT	Computed tomography
EGF	Epidermal growth factor
FAH	Fumarylacetoacetate hydrolase
HT1	Hereditary tyrosinemia type I
MIP	Maximum Intensity Images
NIS	Sodium Iodide Symporter
NTBC	2-(2-nitro-4-trifluoromethylbenzyol)-1,3 cyclohexanedione
PET	Positron emission tomography
SPECT	Single-photon emission computed tomography
SFFV	Spleen focus forming virus

References

1. Fox IJ, Chowdhury JR, Kaufman SS, Goertzen TC, Chowdhury NR, Warkentin PI, Dorko K, et al. Treatment of the Crigler-Najjar syndrome type I with hepatocyte transplantation. N Engl J Med. 1998; 338:1422–1426. [PubMed: 9580649]
2. Dhawan A, Puppi J, Hughes RD, Mitry RR. Human hepatocyte transplantation: current experience and future challenges. Nat Rev Gastroenterol Hepatol. 2010; 7:288–298. [PubMed: 20368738]
3. Huebert RC, Rakela J. Cellular therapy for liver disease. Mayo Clinic proceedings. 2014; 89:414–424. [PubMed: 24582199]
4. Yu Y, Fisher JE, Lillegard JB, Rodysill B, Amiot B, Nyberg SL. Cell therapies for liver diseases. Liver transplantation: official publication of the American Association for the Study of Liver Diseases and the International Liver Transplantation Society. 2012; 18:9–21.
5. Hughes RD, Mitry RR, Dhawan A. Current status of hepatocyte transplantation. Transplantation. 2012; 93:342–347. [PubMed: 22082820]
6. Kroon E, Martinson LA, Kadoya K, Bang AG, Kelly OG, Eliazer S, Young H, et al. Pancreatic endoderm derived from human embryonic stem cells generates glucose-responsive insulin-secreting cells in vivo. Nat Biotech. 2008; 26:443–452.
7. Zhu S, Rezvani M, Harbell J, Mattis AN, Wolfe AR, Benet LZ, Willenbring H, et al. Mouse liver repopulation with hepatocytes generated from human fibroblasts. Nature. 2014; 508:93–97. [PubMed: 24572354]
8. Hoppo T, Komori J, Manohar R, Stolz DB, Lagasse E. Rescue of lethal hepatic failure by hepatized lymph nodes in mice. Gastroenterology. 2011; 140:656–666 e652. [PubMed: 21070777]

9. Penheiter AR, Russell SJ, Carlson SK. The sodium iodide symporter (NIS) as an imaging reporter for gene, viral, and cell-based therapies. Current gene therapy. 2012; 12:33–47. [PubMed: 22263922]
10. Cho JY. A transporter gene (sodium iodide symporter) for dual purposes in gene therapy: imaging and therapy. Current gene therapy. 2002; 2:393–402. [PubMed: 12477251]
11. Lindblad B, Lindstedt S, Steen G. On the enzymic defects in hereditary tyrosinemia. Proc Natl Acad Sci U S A. 1977; 74:4641–4645. [PubMed: 270706]
12. Overturf K, al-Dhalimy M, Ou CN, Finegold M, Grompe M. Serial transplantation reveals the stem-cell-like regenerative potential of adult mouse hepatocytes. Am J Pathol. 1997; 151:1273–1280. [PubMed: 9358753]
13. Grompe M, al-Dhalimy M, Finegold M, Ou CN, Burlingame T, Kennaway NG, Soriano P. Loss of fumarylacetoacetate hydrolase is responsible for the neonatal hepatic dysfunction phenotype of lethal albino mice. Genes Dev. 1993; 7:2298–2307. [PubMed: 8253378]
14. Nelson TJ, Martinez-Fernandez A, Yamada S, Mael AA, Terzic A, Ikeda Y. Induced pluripotent reprogramming from promiscuous human stemness related factors. Clinical and translational science. 2009; 2:118–126. [PubMed: 20161095]
15. Harding CO, Gillingham MB, Hamman K, Clark H, Goebel-Daghighi E, Bird A, Koeberl DD. Complete correction of hyperphenylalaninemia following liver-directed, recombinant AAV2/8 vector-mediated gene therapy in murine phenylketonuria. Gene therapy. 2006; 13:457–462. [PubMed: 16319949]
16. Wang L, Takabe K, Bidlingmaier SM, Ill CR, Verma IM. Sustained correction of bleeding disorder in hemophilia B mice by gene therapy. Proceedings of the National Academy of Sciences of the United States of America. 1999; 96:3906–3910. [PubMed: 10097136]
17. Pinke LA, Dean DS, Bergert ER, Spitzweg C, Dutton CM, Morris JC. Cloning of the mouse sodium iodide symporter. Thyroid: official journal of the American Thyroid Association. 2001; 11:935–939. [PubMed: 11716040]
18. Zufferey R, Nagy D, Mandel RJ, Naldini L, Trono D. Multiply attenuated lentiviral vector achieves efficient gene delivery in vivo. Nature biotechnology. 1997; 15:871–875.
19. Dingli D, Peng KW, Harvey ME, Greipp PR, O'Connor MK, Cattaneo R, Morris JC, et al. Image-guided radiovirotherapy for multiple myeloma using a recombinant measles virus expressing the thyroidal sodium iodide symporter. Blood. 2004; 103:1641–1646. [PubMed: 14604966]
20. van der Have F, Vastenhouw B, Ramakers RM, Branderhorst W, Krah JO, Ji C, Staelens SG, et al. U-SPECT-II: An Ultra-High-Resolution Device for Molecular Small-Animal Imaging. Journal of nuclear medicine: official publication, Society of Nuclear Medicine. 2009; 50:599–605.
21. Vastenhouw B, Beekman F. Submillimeter total-body murine imaging with U-SPECT-I. Journal of nuclear medicine: official publication, Society of Nuclear Medicine. 2007; 48:487–493.
22. Suksanpaisan L, Pham L, McIvor S, Russell SJ, Peng KW. Oral contrast enhances the resolution of in-life NIS reporter gene imaging. Cancer gene therapy. 2013; 20:638–641. [PubMed: 24030210]
23. Branderhorst W, Vastenhouw B, Beekman FJ. Pixel-based subsets for rapid multi-pinhole SPECT reconstruction. Physics in medicine and biology. 2010; 55:2023–2034. [PubMed: 20299722]
24. Wang X, Montini E, Al-Dhalimy M, Lagasse E, Finegold M, Grompe M. Kinetics of liver repopulation after bone marrow transplantation. The American journal of pathology. 2002; 161:565–574. [PubMed: 12163381]
25. Grompe M, Jones SN, Loulseged H, Caskey CT. Retroviral-mediated gene transfer of human ornithine transcarbamylase into primary hepatocytes of spf and spf-ash mice. Human gene therapy. 1992; 3:35–44. [PubMed: 1562638]
26. Ponder KP, Gupta S, Leland F, Darlington G, Finegold M, DeMayo J, Ledley FD, et al. Mouse hepatocytes migrate to liver parenchyma and function indefinitely after intrasplenic transplantation. Proceedings of the National Academy of Sciences of the United States of America. 1991; 88:1217–1221. [PubMed: 1899924]
27. Rothe M, Rittelmeyer I, Iken M, Rudrich U, Schambach A, Glage S, Manns MP, et al. Epidermal growth factor improves lentivirus vector gene transfer into primary mouse hepatocytes. Gene therapy. 2012; 19:425–434. [PubMed: 21850050]

28. Overturf K, Al-Dhalimy M, Tanguay R, Brantly M, Ou CN, Finegold M, Grompe M. Hepatocytes corrected by gene therapy are selected in vivo in a murine model of hereditary tyrosinaemia type I. Nat Genet. 1996; 12:266–273. [PubMed: 8589717]
29. Grompe M, Lindstedt S, al-Dhalimy M, Kennaway NG, Papaconstantinou J, Torres-Ramos CA, Ou CN, et al. Pharmacological correction of neonatal lethal hepatic dysfunction in a murine model of hereditary tyrosinaemia type I. Nat Genet. 1995; 10:453–460. [PubMed: 7545495]
30. Nyberg SL, Hardin J, Amiot B, Argikar UA, Remmel RP, Rinaldo P. Rapid, large-scale formation of porcine hepatocyte spheroids in a novel spheroid reservoir bioartificial liver. Liver transplantation: official publication of the American Association for the Study of Liver Diseases and the International Liver Transplantation Society. 2005; 11:901–910.
31. Landry J, Bernier D, Ouellet C, Goyette R, Marceau N. Spheroidal aggregate culture of rat liver cells: histotypic reorganization, biomatrix deposition, and maintenance of functional activities. The Journal of cell biology. 1985; 101:914–923. [PubMed: 2411740]
32. Brophy CM, Luebke-Wheeler JL, Amiot BP, Khan H, Remmel RP, Rinaldo P, Nyberg SL. Rat hepatocyte spheroids formed by rocked technique maintain differentiated hepatocyte gene expression and function. Hepatology. 2009; 49:578–586. [PubMed: 19085959]
33. Nguyen PK, Riegler J, Wu JC. Stem Cell Imaging: From Bench to Bedside. Cell stem cell. 2014; 14:431–444. [PubMed: 24702995]
34. Contag CH, Contag PR, Mullins JI, Spilman SD, Stevenson DK, Benaron DA. Photonic detection of bacterial pathogens in living hosts. Molecular microbiology. 1995; 18:593–603. [PubMed: 8817482]
35. Turner RA, Wauthier E, Lozoya O, McClelland R, Bowsher JE, Barbier C, Prestwich G, et al. Successful transplantation of human hepatic stem cells with restricted localization to liver using hyaluronan grafts. Hepatology. 2013; 57:775–784. [PubMed: 22996260]
36. Komori J, Boone L, DeWard A, Hoppo T, Lagasse E. The mouse lymph node as an ectopic transplantation site for multiple tissues. Nature Biotechnology. 2012; 30:976. +
37. Chen IY, Wu JC. Cardiovascular molecular imaging: focus on clinical translation. Circulation. 2011; 123:425–443. [PubMed: 21282520]
38. Luker GD, Luker KE. Optical imaging: current applications and future directions. Journal of nuclear medicine: official publication, Society of Nuclear Medicine. 2008; 49:1–4.
39. Hickey RD, Lillegard JB, Fisher JE, McKenzie TJ, Hofherr SE, Finegold MJ, Nyberg SL, et al. Efficient production of Fah-null heterozygote pigs by chimeric adeno-associated virus-mediated gene knockout and somatic cell nuclear transfer. Hepatology. 2011; 54:1351–1359. [PubMed: 21674562]
40. Hickey RD, Mao SA, Glorioso J, Lillegard JB, Fisher JE, Amiot B, Rinaldo P, et al. Fumarylacetoacetate hydrolase deficient pigs are a novel large animal model of metabolic liver disease. Stem cell research. 2014; 13:144–153. [PubMed: 24879068]
41. Rogers CS, Stoltz DA, Meyerholz DK, Ostedgaard LS, Rokhlina T, Taft PJ, Rogan MP, et al. Disruption of the CFTR gene produces a model of cystic fibrosis in newborn pigs. Science. 2008; 321:1837–1841. [PubMed: 18818360]
42. Gupta S, Lee CD, Vemuru RP, Bhargava KK. 111Indium labeling of hepatocytes for analysis of short-term biodistribution of transplanted cells. Hepatology. 1994; 19:750–757. [PubMed: 8119703]
43. Cheng K, Benten D, Bhargava K, Inada M, Joseph B, Palestro C, Gupta S. Hepatic targeting and biodistribution of human fetal liver stem/progenitor cells and adult hepatocytes in mice. Hepatology. 2009; 50:1194–1203. [PubMed: 19637284]
44. Defresne F, Tondreau T, Stephenne X, Smets F, Bourgois A, Najimi M, Jamar F, et al. Biodistribution of adult derived human liver stem cells following intraportal infusion in a 17-year-old patient with glycogenosis type 1A. Nuclear medicine and biology. 2014; 41:371–375. [PubMed: 24607438]
45. Bohnen NI, Charron M, Reyes J, Rubinstein W, Strom SC, Swanson D, Towbin R. Use of indium-111-labeled hepatocytes to determine the biodistribution of transplanted hepatocytes through portal vein infusion. Clinical Nuclear Medicine. 2000; 25:447–450. [PubMed: 10836694]

46. Templin C, Zweigerdt R, Schwanke K, Olmer R, Ghadri JR, Emmert MY, Muller E, et al. Transplantation and tracking of human-induced pluripotent stem cells in a pig model of myocardial infarction: assessment of cell survival, engraftment, and distribution by hybrid single photon emission computed tomography/computed tomography of sodium iodide symporter transgene expression. Circulation. 2012; 126:430–439. [PubMed: 22767659]

47. Russell SJ, Federspiel MJ, Peng KW, Tong C, Dingli D, Morice WG, Lowe V, et al. Remission of disseminated cancer after systemic oncolytic virotherapy. Mayo Clinic proceedings. 2014; 89:926–933. [PubMed: 24835528]

48. Wangensteen KJ, Wilber A, Keng VW, He Z, Matise I, Wangensteen L, Carson CM, et al. A facile method for somatic, lifelong manipulation of multiple genes in the mouse liver. Hepatology. 2008; 47:1714–1724. [PubMed: 18435462]

49. Wilber A, Wangensteen KJ, Chen YX, Zhuo LJ, Frandsen JL, Bell JB, Chen ZYJ, et al. Messenger RNA as a source of transposase for Sleeping Beauty transposon-mediated correction of hereditary tyrosinemia type I. Molecular Therapy. 2007; 15:1280–1287. [PubMed: 17440442]

50. Moolten FL. Tumor chemosensitivity conferred by inserted herpes thymidine kinase genes: paradigm for a prospective cancer control strategy. Cancer research. 1986; 46:5276–5281. [PubMed: 3019523]

51. Di Stasi A, Tey SK, Dotti G, Fujita Y, Kennedy-Nasser A, Martinez C, Straathof K, et al. Inducible Apoptosis as a Safety Switch for Adoptive Cell Therapy. New England Journal of Medicine. 2011; 365:1673–1683. [PubMed: 22047558]

52. Wilson JM, Johnston DE, Jefferson DM, Mulligan RC. Correction of the genetic defect in hepatocytes from the Watanabe heritable hyperlipidemic rabbit. Proc Natl Acad Sci U S A. 1988; 85:4421–4425. [PubMed: 2454468]

53. Matas AJ, Sutherland DE, Steffes MW, Mauer SM, Sowe A, Simmons RL, Najarian JS. Hepatocellular transplantation for metabolic deficiencies: decrease of plasms bilirubin in Gunn rats. Science. 1976; 192:892–894. [PubMed: 818706]

54. Yamanouchi K, Zhou H, Roy-Chowdhury N, Macaluso F, Liu L, Yamamoto T, Yannam GR, et al. Hepatic irradiation augments engraftment of donor cells following hepatocyte transplantation. Hepatology. 2009; 49:258–267. [PubMed: 19003915]

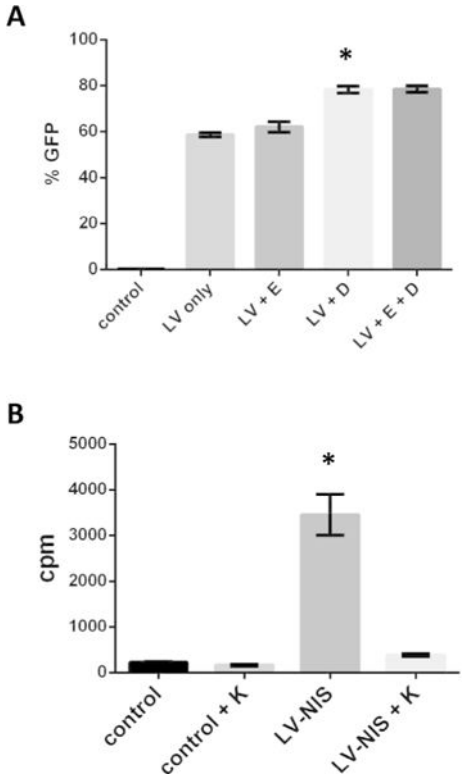

Figure 1.

Ex vivo transduction of primary hepatocytes. (A) Quantification of flow cytometry data based on GFP expression after lentiviral vector transduction of hepatocytes with LV-TBG-GFP with or without the addition of EGF [E] and dexamethasone [D]. *P<0.01. (B) In vitro radiolabeled iodine (I-125) uptake assay showing a significant increase in I-125 uptake in LV-TBG-NIS transduced hepatocytes. I-125 uptake in LV-TBG-NIS transduced hepatocytes was blocked with the addition of potassium perchlorate (K). *P<0.01.

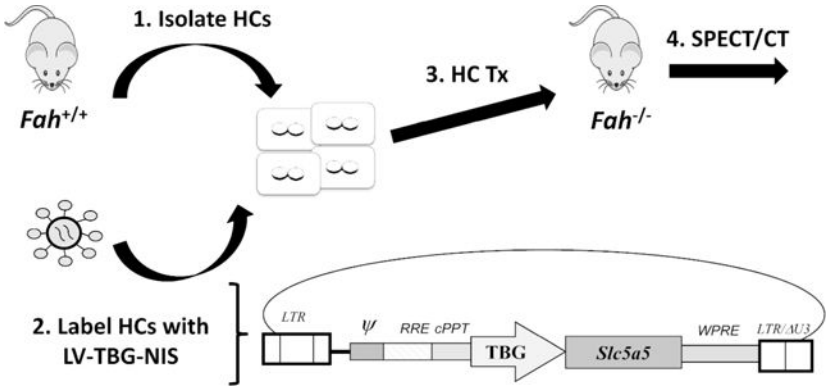

Figure 2.

Summary of in vivo hepatocyte transplantation procedure. Hepatocytes (HC) were transduced with a lentiviral vector expressing NIS prior to transplantation (Tx). A schematic of the vector is also included that contained the NIS gene (*Slc5a5*).

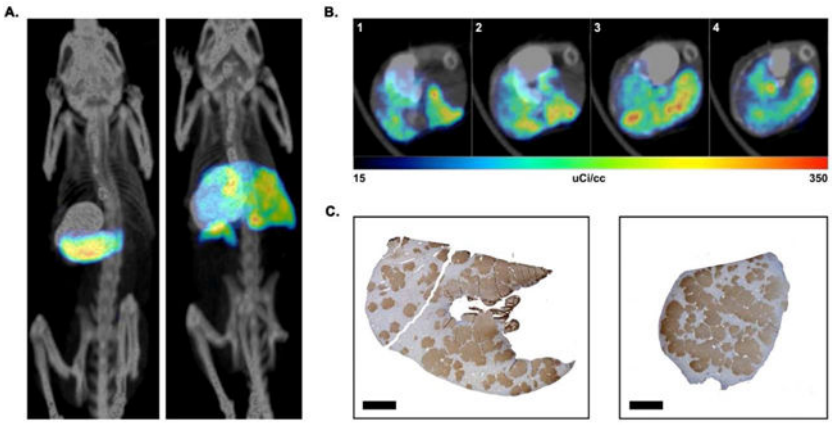

Figure 3.

In vivo imaging of NIS-labeled hepatocytes. (A) Representative fused Maximum Intensity Images (MIP) images of control hepatocyte injected (left) and NIS-labeled hepatocyte injected (right) mice. The location of the stomach was identified by oral administration of barium sulfate prior to imaging. The signals from the thyroid and bladder have been removed from both animals. (B) Representative transverse SPECT/CT sections of a NIS-labeled hepatocyte transplanted liver, showing different positions of the liver from head [1] to feet [4] of animal. (C) FAH-immunohistochemistry of the same liver showing non-uniform distribution of transplanted cells in two different lobes from the same mouse. FAH-positive cells are stained brown. Scale bar = 2mm.

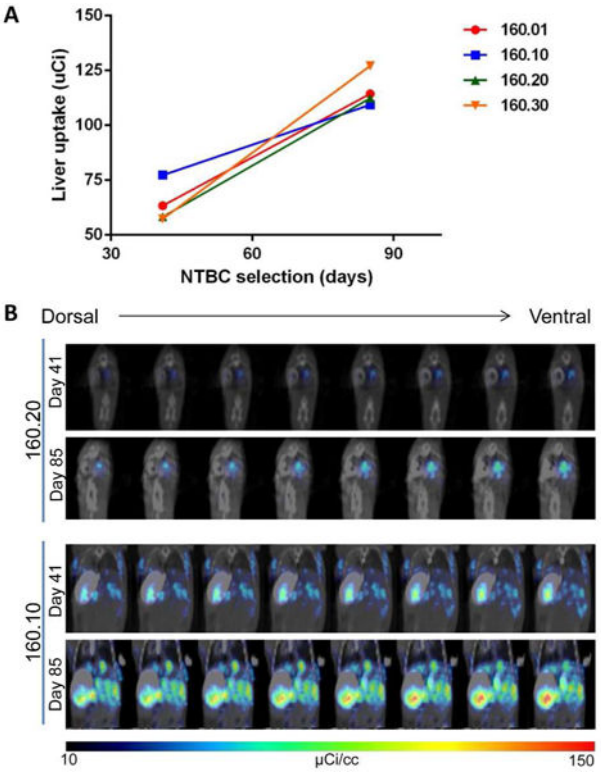

Figure 4.

Longitudinal imaging of individual transplanted mice. (A) Quantification of liver uptake of technetium-99m-pertechnetate in four mice transplanted with NIS-labeled cells. Mice were imaged after 41 and 85 days of NTBC selection. (B) Representative images from two mice (160.10 & 160.20) showing an increase in technetium-99m-pertechnetate uptake in the liver over time. Eight serial sections through similar locations at the two time points were used to demonstrate the regeneration of individual cell clusters over time.

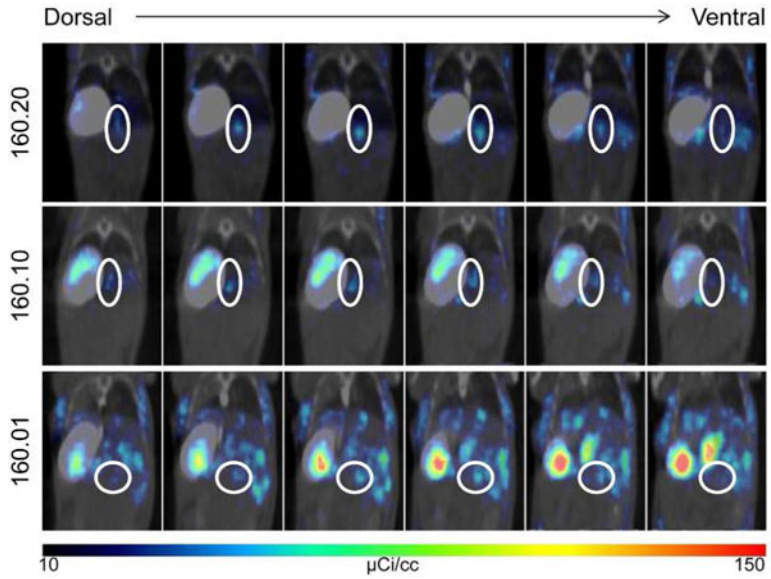

Figure 5.

High resolution imaging of individual regenerating nodules. Near-serial SPECT/CT sections through individual nodules in three separate mice show increasing and then decreasing nodule diameter and uptake at day 41 of NTBC selection. White ovals highlight the individual nodule being followed. The location of the stomach was identified by oral administration of barium sulfate prior to imaging.

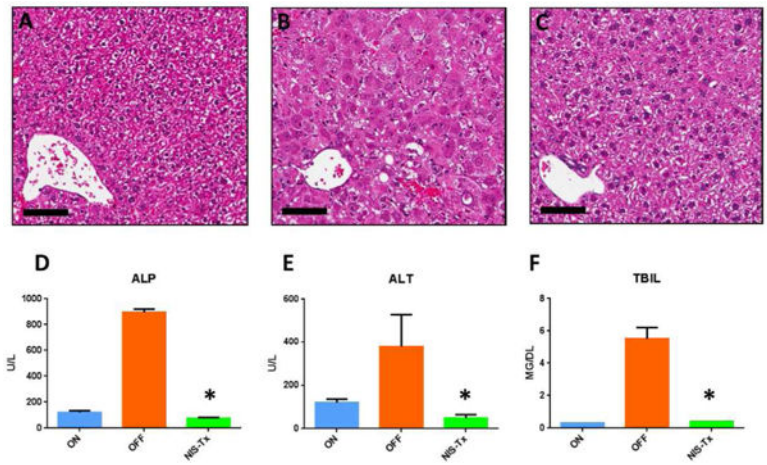

Figure 6.

NIS-labeling does not impact hepatocyte biology. (A–C) Representative images of H&E stained livers of *Fah*$^{-/-}$ mice on NTBC (A), off NTBC (B), and after repopulation with NIS-labeled hepatocytes (C). Scale bar = 80 um. (D–F) Biochemical analysis of levels of plasma alkaline phosphatase, alanine aminotransferase and total bilirubin of *Fah*$^{-/-}$ mice on NTBC (left), off NTBC (middle), and after repopulation with NIS-labeled hepatocytes (right). *P<0.01.

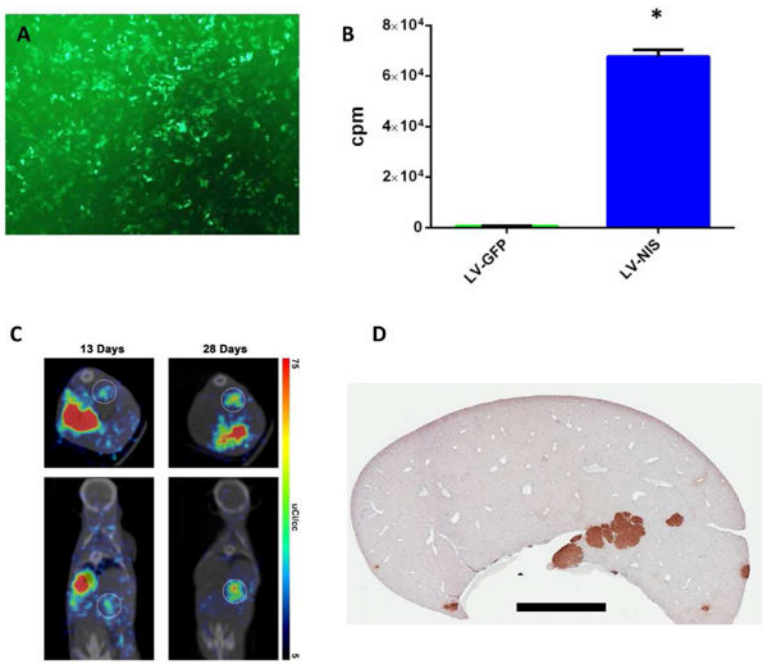

Figure 7.

Hepatocyte spheroids can engraft in vivo. (A) Detection of GFP-positive cells in vitro after transduction of hepatocytes during rocked spheroid formation. (B) In vitro radiolabeled iodine (I-125) uptake assay showing a significant increase in LV-TBG-NIS transduced spheroids compared to control LV-TBG-GFP transduced spheroids. *P<0.01. (C) Representative images after 13 (left) and 28 days (right) of a single mouse injected with NIS-labeled spheroids. In the right image, the signal from the stomach is masked using barium sulfate administration. (D) FAH-immunohistochemistry of the same liver showing donor FAH-positive cells (stained brown) integrated in the liver parenchyma. Scale bar = 2mm.